The inhibitory effects of class I histone deacetylases on hippocampal neuroinflammatory regulation in aging mice with postoperative cognitive dysfunction

C.-X. YANG¹, F. BAO¹, J. ZHONG², L. ZHANG¹, L.-B. DENG¹, Q. SHA¹, H. JIANG¹

¹Department of Anesthesiology, Qingpu Branch of Zhongshan, Fudan University, Shanghai, China ²Department of Anesthesiology, Jinshan Hospital, Fudan University, Shanghai, People's Republic of China

Abstract. – OBJECTIVE: Neuroinflammation in the hippocampus has been determined to contribute to postoperative cognitive dysfunction (POCD) occurrence in elderly individuals. Histone deacetylases (HDACs) have been identified as important regulators of inflammation. However, the roles of different types of HDACs in POCD have never been fully explored.

MATERIALS AND METHODS: POCD mouse models were established using isoflurane and validated by the Morris water maze test. The mice were pretreated with UF010 [a Class I HDAC inhibitor (HDACi)], MC1568 (a Class II HDACi) and SAHA (a Class I and II HDACi) before POCD establishment. HDAC protein levels and the activity of the NF-κB/p65, JAK/STAT and TLR/MyD88 signaling pathways in the hippocampus were investigated by Western blot (WB). The enrichment of HDACs on the promoters of genes was detected using ChIP-qPCR.

RESULTS: Class I HDACs, including HDAC2 and HDAC8, and Class II HDACs, including HDAC4, HDAC7 and HDAC10, were all upregulated in the POCD group compared to the control group. Furthermore, compared to the MC1568 pretreatment group and the control group, the groups pretreated with UF010 and SAHA exhibited amelioration of the effects of anesthesia/ surgery induced POCD and compromised inflammatory reactions in the hippocampus. Likewise, the NF-kB/p65, JAK/STAT and TLR/MyD88 signaling pathways were inactivated upon pretreatment with UF010 and SAHA compared to MC1568. Finally, the transcription of the genes negatively regulating these three pathways declined, and the enrichment of HDAC1, HDAC2 and HDAC8 was significantly elevated in the context of POCD.

CONCLUSIONS: Class I HDACs, especially HDAC1, HDAC2 and HDAC8, play crucial roles in enhancing neuroinflammation in the hippocampus and causing POCD. Class I HDACs are potential therapeutic targets for POCD prevention and treatment *via* neuroinflammation inhibition.

Key Words: POCD, Inflammation, HDAC, HDACi.

Introduction

Postoperative cognitive dysfunction (POCD) is a clinical syndrome associated with perioperative reversible mental disorders, including cognitive dysfunction, memory impairment, anxiety, personality changes and mental confusion, in patients after surgery under volatile anesthetics. POCD diminishes patients' quality of life and increases social dependence, the likelihood of postoperative complications and the risk for postoperative mortality¹.

Inhaled sevoflurane can promote the progression of cognitive dysfunction in the elderly population, especially in individuals over 65 years old²⁻⁴. One of the underlying mechanisms of the pathogenesis of POCD involves the release of multiple inflammatory factors and cytokines due to microglia-mediated overactive neuroinflammation that further enhances the injury of neurons in the hippocampus. Despite the recent improvements in interventional strategies targeting inflammation in POCD, simple anti-inflammatory treatments fail to provide curative effects. Classic signaling pathways, such as the nuclear factor of kappa light polypeptide gene enhancer in B cells/RELA proto-oncogene, NFkB subunit (NF-κB/p65)⁵, Janus kinase/signal transducer and activator of transcription (JAK/ STAT)⁶ and toll-like receptor/myeloid differentiation primary response gene 88 (TLR/MyD88)⁷ pathways, play critical roles in inflammatory responses and the inflammation-induced cognitive impairment process. Thus, the development of better therapeutic targets that inhibit the above endogenous signaling pathways involved in cerebral neuroinflammation will be of great significance in the field of neurobiology.

Histone deacetylases (HDACs) contribute to the maintenance of histone acetylation on genomic DNA in coordination with histone acetyltransferases (HATs), and their dysregulation is connected with multiple human diseases. Based on their different protein structures, HDAC family members can be divided into four distinct groups: Class I (HDAC1, HDAC2, HDAC3, HDAC8), Class IIa (HDAC4, HDAC5, HDAC7, HDAC9), Class IIb (HDAC6, HDAC10), Class III (Silent information regulator factor 2-related enzyme 1, SIRT1) and Class IV (HDAC11). Although HDACs play roles in regulating histone deacetylation and gene silencing, the differences in target genes among HDAC members have rarely been explored. Previous studies have revealed that Class I HDACs play essential roles in inflammatory disorders related to POCD via NFκB/p65 inhibition⁸. On the other hand, the other classes of HDACs have also been determined to be closely connected with inflammation-associated regulatory pathways. Thus, determining the patterns and roles of different HDACs in the pathogenesis of POCD was the objective of this study. The results of our investigation extend the underlying mechanism of POCD and provide insights into effective HDAC-targeting therapies for POCD.

Materials and Methods

Animal Study

C57BL/6 (18 months old) male mice were obtained from SLAC Laboratory Animal Co., Ltd. (Shanghai, China). The animals were kept in a pathogen-free environment with a laminar flow system and maintained at 22 ± 2 °C with a constant 12-hour light/dark schedule. The animals were allowed free access to food and water. The studies were conducted in accordance with the Animal Component of Research Protocol guidelines at Fudan University. The mice were randomly assigned to five groups. The negative control (NC) group contained ten individuals without any intervention that were used as negative controls. In the POCD group, as previously described9, fifty individuals were placed in a transparent chamber fitted with a $30 \times 15 \times 15$

cm³ vaporizer and kept anesthetized with 3% isoflurane for 6 hours before undergoing pure oxygen treatment. After the mice were woken naturally, the POCD mice were evaluated by the Morris water maze test and used for the next experiments. The last three groups were the UF010 (UF), SAHA and MC1568 (MC) groups. Fifty individuals each in the UF, SAHA, and MC groups were intraperitoneally administered 15 mg/kg UF010, 20 mg/kg 4-iodo-SAHA and 20 mg/kg MC1568 (APExBIO, Houston, TX, USA), respectively, for 0.5 h of pretreatment before POCD model preparation⁸. For these pretreatment groups, behavioral examinations were not conducted; the animals were directly sacrificed for the next experiments because the rate of isoflurane induced POCD did not reach 100% and because we failed to identify the non-POCD individuals. These issues were probably related to the natural probability of POCD induction or HDAC inhibitor (HDACi) pretreatment effects.

The Morris water maze test was used to verify the successful establishment of the POCD model as indicated previously¹⁰. Briefly, a platform was initially set in the center of a pool 0.5 m in height and 1.2 m in diameter at a level 5 cm higher than the water surface. Mice were trained at the same entrance for a total of 2 min per trial from the 2nd to the 7th day after isoflurane treatment. The path taken, the escape time and the distance were all recorded.

Western Blot (WB) Assay

Hippocampus samples were homogenized in radioimmunoprecipitation assay (RIPA) buffer solution (Beyotime Biotechnology, Nantong, Jiangsu, China), and then, centrifuged at 4°C at 13,000 rpm for 10 min. The protein quantity in the supernatant was determined using a bicinchoninic acid (BCA) protein assay kit (Sango, Shanghai, China). Equal amounts of protein samples were separated by sodium dodecyl sulfate-polyacrylamide gel electrophoresis (SDS-PAGE) and transferred to polyvinylidene difluoride membranes. The membranes were blocked with 5% nonfat milk in TBS for 90 min, and then, incubated with primary antibodies against Histone H3ac (1:2000, AB 2687871, Activemotif, Carlsbad, CA, USA), HDAC1 (1:2000, #34589, CST, Beverly, MA, USA), HDAC2 (1:2000, #5113, CST), HDAC3 (1:2000, #85057, CST, Beverly, MA, USA), HDAC4 (1:2000, #5392, CST, Beverly, MA, USA), HDAC5 (1:2000, #20458, CST, Bever-

ly, MA, USA), HDAC6 (1:2000, #7612, CST, Beverly, MA, USA), HDAC7 (1:2000, #33418, CST, Beverly, MA, USA), HDAC8 (1:2000, ab187139, Abcam, Cambridge, MA, USA), HDAC9 (1:2000, ab59718, Abcam, Cambridge, MA, USA), HDAC10 (1:2000, ab108934, Abcam, Cambridge, MA, USA), HDAC11 (1:2000, ab18973, Abcam, Cambridge, MA, USA), SIRT1 (1:2000, #8469, CST, Beverly, MA, USA), JAK2 (1:2000, #3230, CST, Beverly, MA, USA), p-JAK2 (1:2000, #3771, CST, Beverly, MA, USA), STAT3 (1:2000, #9139, CST, Beverly, MA, USA), p-STAT3 (1:2000, #9145, CST, Beverly, MA, USA), IκBα (1:2000, #4814, CST, Beverly, MA, USA), p65 (1:2000, #8242, CST, Beverly, MA, USA), p-p65 (1:2000, #3033, CST, Beverly, MA, USA), TLR4 (1:2000, #14358, CST, Beverly, MA, USA), MyD88 (1:2000, #4283, CST, Beverly, MA, USA) and GAPDH (1:5000, Beyotime Biotechnology, Shanghai, China) overnight at 4°C. The membranes were washed in TBST and incubated with HRP-conjugated rabbit anti-mouse and goat anti-rabbit IgG (1:20000 dilution, Beyotime Biotechnology, Shanghai, China) at room temperature (RT) for 1 h. The membranes were then treated with an enhanced chemiluminescence detection kit (ECL; Millipore, Billerica, MA, USA), and the intensity of each band was quantified by a Tanon 4600SF system (Tanon, Shanghai, China).

Enzyme-Linked Immunosorbent Assay (ELISA)

Interleukin 6 (IL-6), C-reactive protein (CRP), and tumor necrosis factor alpha (TNF- α) levels in serum and hippocampal tissues were detected using ELISA kits (Thermo Fisher Scientific, Waltham, MA, USA) according to the manufacturer's instructions.

Flow Cytometry (FACS)

Hippocampus samples were digested with 0.1 mg/ml collagenase IV and 2 mg/ml papain (Millipore, Billerica, MA, USA) at 37°C for 20 min and gently passed through a 70 μ m strainer. Next, the samples were washed twice with PBS, resuspended in 5 ml of 70% Percoll (GE Healthcare Life Sciences, Pittsburgh, PA, USA), gently treated with 37% Percoll, and centrifuged at 500 μ g for 30 min. The cell layer between the 37% and 70% Percoll was harvested and incubated with the appropriate antibodies (1:50) on ice for 15 min in the dark. The flow cytometry samples were all stained with 1 μ l of 50 μ g/ml propidium

iodide (PI; Millipore, Billerica, MA, USA) for 5 min. Antibodies against all of the following proteins were purchased from Thermo Fisher Scientific (Waltham, MA, USA): CD3 (FITC, 11-0031-82), CD4 (PE, 12-0041-82), and NK1.1 (PE, 17-5941-82). All PI-negative cells were defined as the following cell types: NK cells (CD3–NK1.1+) and CD4 T cells (CD3+CD4+).

Chromatin Immunoprecipitation (ChIP) Assay

Briefly, 107 cells were fixed with 1% formaldehyde, quenched with 0.125 M glycine at room temperature, and then, lysed in 500 µl of lysis buffer [10 mM Tris-HCl (pH 8.0)], 10 mM NaCl, and 0.2% IGEPAL CA-630 (Thermo Fisher Scientific, Waltham, MA, USA) on ice for 30 min. The genomic DNA was sonicated into 200-500 bp. Ten percent of each whole-cell lysate was stored as input, and the rest of the lysate was incubated with 1 µg of the appropriate primary antibodies at 4°C overnight. Then, an additional 2-hour pull-down was performed at 4°C with protein-A beads (Thermo Fisher Scientific, Waltham, MA, USA). Primers (Table I) designed to encompass approximately 150 bp around the target regions were used to detect the enrichment of HDACs using qPCR.

Quantitative PCR (qPCR) Assay

RNA was extracted using TRIzol, quantified with a NanoDrop (Thermo Fisher Scientific, Waltham, MA, USA), and converted to cDNA using a reverse transcription kit (Roche, Basel, Switzerland). The templates were detected using Fast Universal SYBR Green Real-time PCR Master Mix (Roche, Basel, Switzerland) under the following conditions: 95°C/2 min and 50 cycles of 95°C/15 seconds, 55°C/15 seconds, 72°C/1 min, and 72°C/10 min. The primers used in this study are listed in **Supplementary Table I**.

Statistical Analysis

All statistical analyses were conducted in SPSS 20 (IBM Corp., Armonk, NY, USA). For qPCR data, the 2^{Δ} method was used to calculate the expression, enrichment or probable DNA contact. Student's *t*-test was used to evaluate differences between groups. The χ^2 square test was used to assess differences between genes negatively regulating and positively regulating inflammatory signaling pathways. A *p*-value less than 0.05 was considered to indicate a significant difference.

A heatmap was prepared using our qPCR data and described using the pheatmap package of RStudio.

Results

Characterization of HDAC Expression in the Hippocampus in POCD

Initially, a POCD mouse model was established using isoflurane as previously described⁹. The behavioral phenotype was assessed daily from the 2nd to the 7th day post induction by Morris water maze examination. Thirteen of fifty mice that displayed an increased escape latency (Figure 1A) and reduced number of crossings (Figure 1B) from the 4th to the 7th day were identified as having POCD. Furthermore, HDAC protein levels in the hippocampus were investigated using Western blot (WB) (Figure 1C, D). Class I HDACs, including HDAC2 and HDAC8, and Class II HDACs, including HDAC4, HDAC7 and HDAC10, were upregulated in the POCD group, while SIRT1 was downregulated in the POCD group compared to the NC group. No significant differences in HDAC11 or other HDACs were observed. Additionally, histone H3ac levels were detected, and we observed that overall histone acetylation was compromised in the hippocampus in the POCD group compared to the NC group. However, a change in HDACs similar to that in the hippocampus failed to occur in the cerebral cortex or amygdala. Overall, our study revealed abnormal changes in HDACs in the hippocampi of POCD mice.

Analysis of Anti-Inflammatory Properties of Class I HDACis Via Pretreatment

Furthermore, HDACis, including UF010 (a Class I HDACi), MC1568 (a Class II HDACi) and SAHA (a Class I and II HDACi), were used to pretreat mice before the POCD model was established. The FACS assay showed that the infiltration of CD4+ T cells (Figure 2A, B) and NK cells (Figure 2C, D) in hippocampal tissues was weakened in the UF010-pretreated and SAHA-pretreated groups compared to the MC1568-pretreated and POCD groups. Consistently, inflammatory parameters, such as interleukin 6 (IL-6), C-reactive protein (CRP), and tumor necrosis factor alpha (TNF-α) levels, in serum and hippocampal tissues were also reduced in the UF010-pretreated and SAHA-pretreated groups

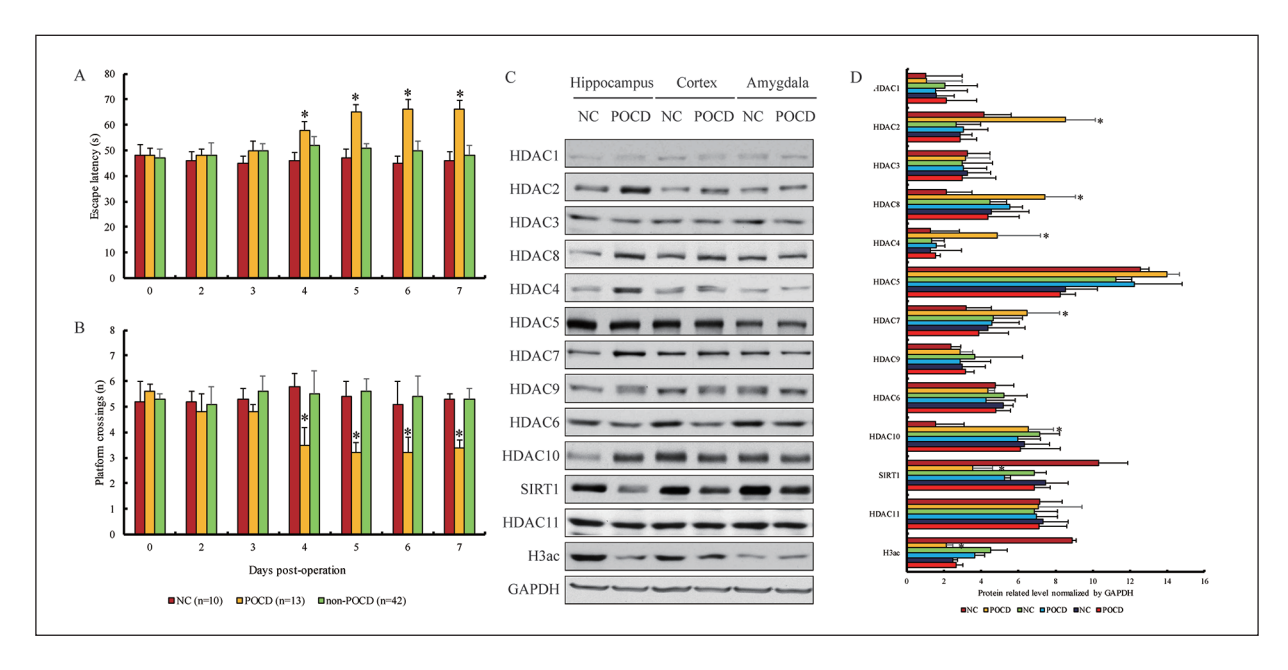


Figure 1. Characterization of HDAC expression in the hippocampi of POCD mice. The escape latency periods (**A**) and numbers of grid crossings (**B**) of POCD mice as examined by the Morris water maze test. The data are presented as the mean \pm standard error of the mean for 65 mice. One-way ANOVA followed by a post hoc test was used. The expression of HDACs in the hippocampus, cerebral cortex and amygdala in POCD was examined by WB assay (**C**) and grayscale value analysis (**D**). The grayscale value is defined as the mean of the integrated optical density of the pixels in the selection. The data are presented as the mean \pm standard error of the mean from three individual experiments. *p<0.05 vs. the NC group.

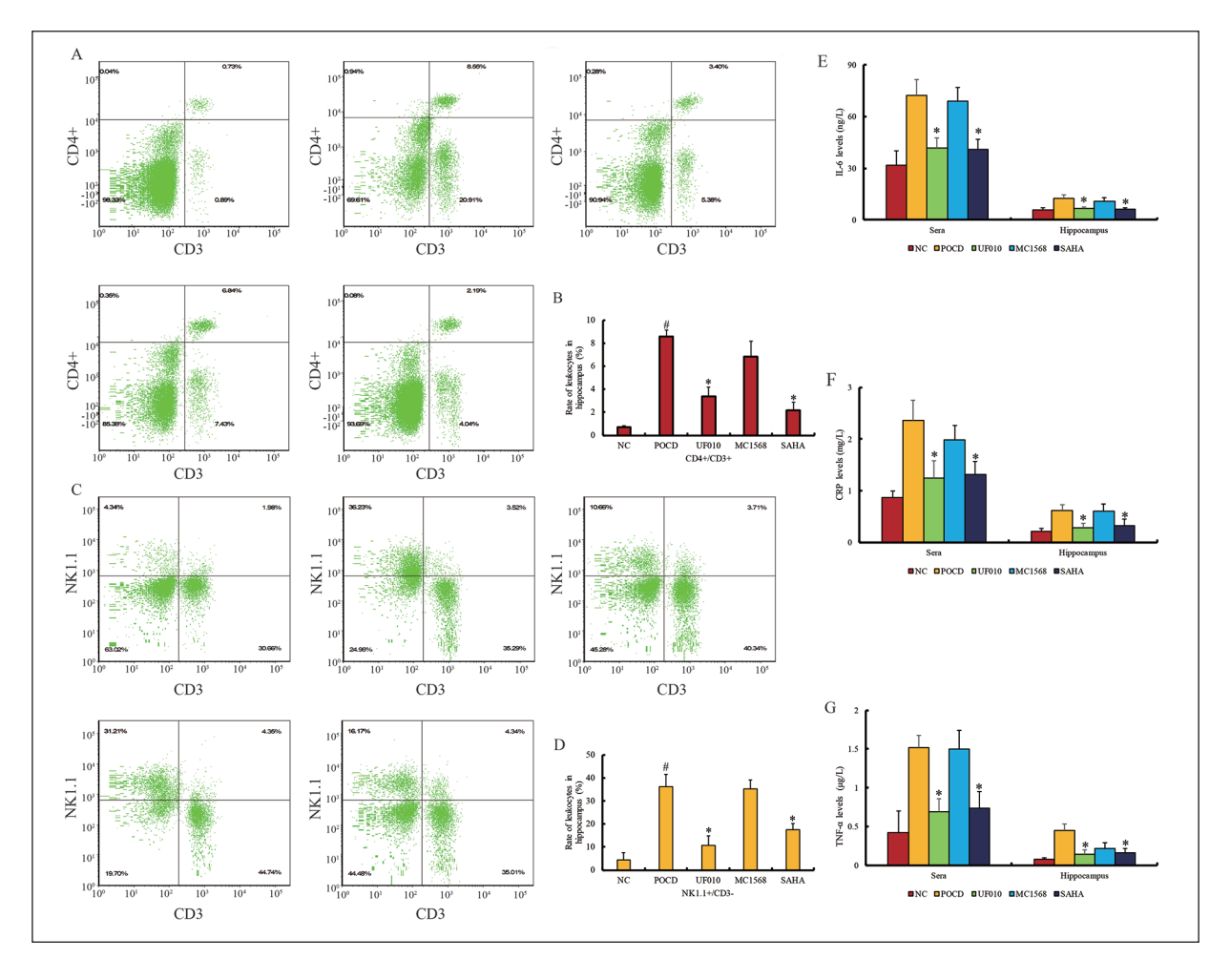


Figure 2. Inflammatory effects in POCD mice treated with HDACis. Flow cytometry sorting of CD4-positive T cells (**A**) and NK cells (**C**) and the results of statistical analysis for these cells (**B**, **D**) from the hippocampi of POCD mice treated with HDACis. Serum levels of interleukin 6 (IL-6) (**E**), C-reactive protein (CRP) (**F**) and tumor necrosis factor alpha (TNF- α) (**G**) in POCD mice treated with HDACis. The data are presented as the mean \pm standard error of the mean from three individual experiments. #p<0.05 vs. the NC group and *p<0.05 vs. the POCD group.

(Figure 2E-G), which indicates that the inflammatory effects of POCD are effectively alleviated by Class I HDACs.

NF-kB/p65, JAK/STAT and TLR/MyD88 Signaling Pathway Inactivation is Regulated by Class I HDACis in POCD

Next, we tried to determine the corresponding signaling pathways for inflammatory regulation. Classic pathways involved in inflammation, including the NF- κ B/p65, JAK/STAT and TLR/MyD88 pathways, were investigated. We observed that all three pathways were markedly activated in the POCD group compared to the NC group but were less activated in the UF010 and SAHA pretreatment groups than in the MC1568 pretreatment and POCD groups

(Figure 3). The results above suggest that Class I HDACs contribute considerably to the inflammatory regulation of hippocampal neurons in POCD.

Transcription of Inflammation-Associated Genes is Regulated by Class I HDACs in POCD

To investigate the transcriptional regulatory roles of HDACs in inflammation, we collected data on a total of 970 genes associated with the NF-κB/p65 (48 terms, 585 genes), JAK/STAT (29 terms, 404 genes) and TLR/MyD88 (13 terms, 59 genes) pathways from the AmiGO 2 database (http://amigo.geneontology.org/amigo). Seventy-seven genes overlapped across these three pathways (Figure 4A). We further investigat-

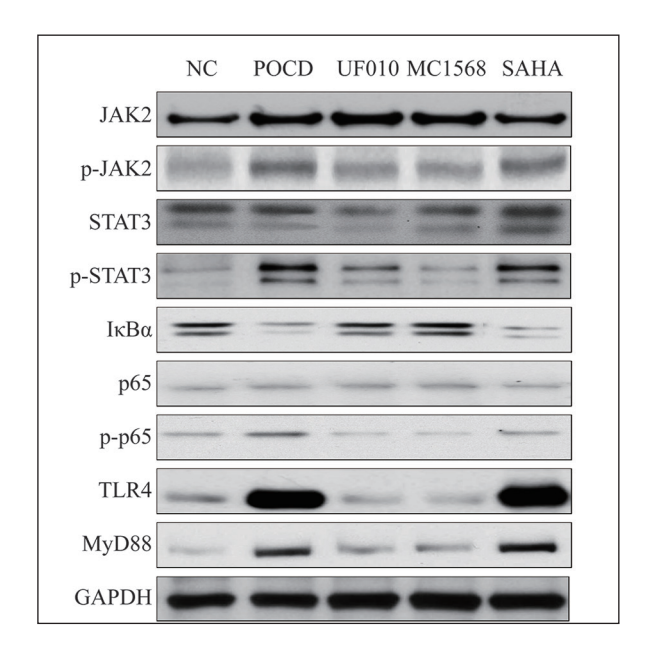


Figure 3. Activity of the JAK/STAT, NF- κ B/p65 and TLR/MyD88 signaling pathways in the hippocampus after treatment with HDACis. The WB assay was performed three separate times.

ed the patterns of HDAC (HDAC1, HDAC2, HDAC3, HDAC4, HDAC6, HDAC8, HDAC9) enrichment on the promoter regions of these 970 genes in published ChIP-seq data from multiple human tissues and cell lines without any drug or genetic editing treatment (Supplementary Table II). The HDAC enrichment data were normalized and are shown in Figure 4B. We observed that HDAC1, HDAC2 and HDAC8 were more highly enriched in the promoters of genes associated with these three pathways than HDAC3, HDAC4, HDAC6 and HDAC9 (p=3.0817E-302) (Figure 4C) and that Class I HDACs contributed considerably to the transcriptional activity of the genes associated with inflammatory signaling pathways (Figure 4D-F). We also observed that, compared to genes involved in the positive regulation of inflammatory activation, 182 genes participating in the negative regulation of NF-κB/p65, JAK/STAT and TLR/MyD88 pathway activation were highly enriched for HDAC1 ($\chi^2=12.541$, p=0.0037), HDAC2 ($\chi^2=16.277$, p=0.0028) and HDAC8 (χ^2 =14.782, p=0.0046).

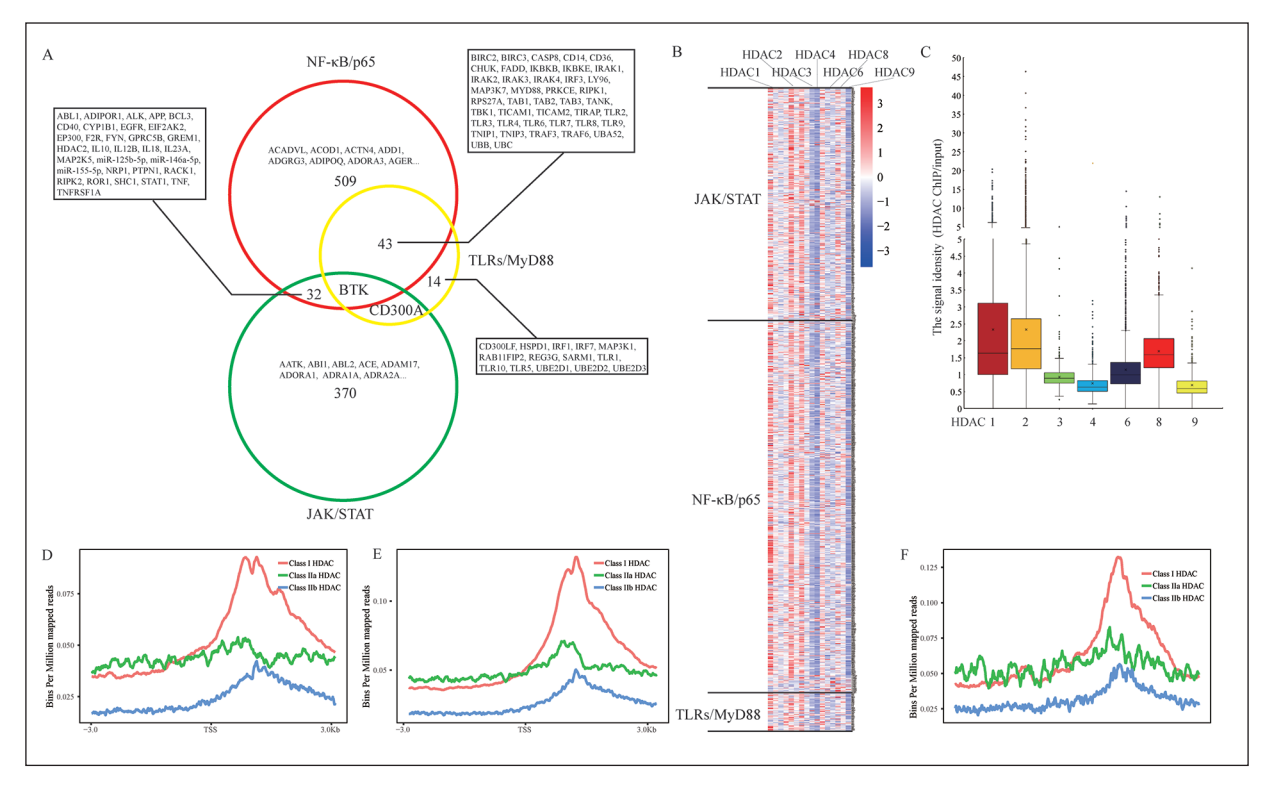


Figure 4. Transcriptional regulation of HDACs in genes associated with inflammation signaling pathways from published ChIP-seq data. Overview of 970 genes associated with the JAK/STAT, NF-κB/p65 and TLR/MyD88 pathways (**A**). Heatmap (**B**) and a box plot (**C**) of HDAC enrichment on the promoter regions of the 970 genes (**B**). The enrichment values are standardized with z-scores, and the colors represent the standardized values, as shown in the color bar. The average enrichment of Class I, IIa and IIb HDACs in the JAK/STAT (**D**), NF-κB/p65 (**E**) and TLR/MyD88 pathways (**F**), measured in bins per million mapped reads, is shown within genomic regions covering 3 kb up- and downstream of the transcription start site (TSS).

Finally, several genes reported to play anti-inflammatory roles, such as adiponectin receptor 1 (ADIPOR1)¹¹, CD300A molecule (CD300A)¹², miR-155-5p, suppressor of cytokine signaling 1 (SOCS1)¹³, protein tyrosine phosphatase nonreceptor type 2 (PTPN2)14 and sterile alpha and HEAT/Armadillo motif containing 1 (SARM1)¹⁵, were selected for further study. We validated the genomic binding preferences of the different HDACs in our POCD mouse model using ChIP-qPCR and validated the transcript levels of these HDACs using qPCR. We observed that the promoters of these genes were highly enriched for HDAC1, HDAC2 and HDAC8 but not for HDAC3, HDAC4, HDAC6 or HDAC9 in the hippocampus in POCD (Figure 5A-G), and the mRNA levels of these six genes were also all reduced in the hippocampus in the POCD group compared to the NC group (Figure 5H). Taken together, our data reveal a transcriptional regulatory role of HDACs in modulating inflammation in POCD.

Discussion

POCD is a common complication of the central nervous system after surgery, but there are few therapeutic options available to prevent it. POCD results in cognitive and behavioral impairment by damaging the hippocampus, which plays specific and fundamental roles in learning, memory and cognition. Due to the long-term effects of exposure to surgical or narcotic stress on the structure and function of the hippocampus, POCD may also cause irreversible disability in patients¹⁶. The hippocampal inflammatory response is the main mechanism involved in the pathogenesis of POCD¹⁷. Kong et al18 have reported that anesthesia/surgery-induced trauma enhances activation of the NF-κB but not the JAK/STAT or TLR/MyD88 signaling pathway. The NF-κB/65 pathway is speculated to be the only pathway for inflammatory activation in POCD, but there is insufficient evidence to support this hypothesis.

HDACs display specific expression patterns associated with specific tissues, cellular locations and functions in different tissues. The expression of HDACs clearly differs among various monoaminergic and neuropeptidergic neuronal groups¹⁹. Class I HDACs are generally restricted to the nucleus and impose transcriptional control, while Class II HDACs move between the nuclear membrane and cytoplasm and are governed by phosphorylation²⁰. The observed changes in HDAC2, HDAC4, HDAC7, HDAC8, HDAC10 and SIRT1 levels in POCD (Figure 1C, D) indicate that compared to the cerebral cortex and amygdala, the hippocampus is severely

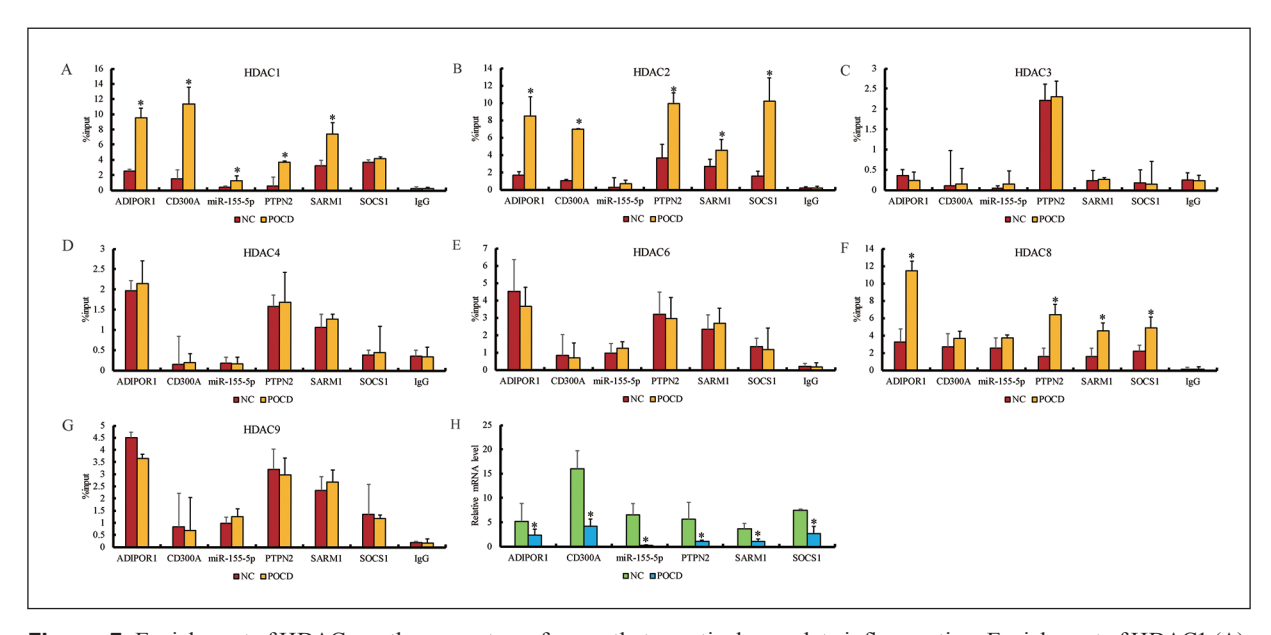


Figure 5. Enrichment of HDACs on the promoters of genes that negatively regulate inflammation. Enrichment of HDAC1 (**A**), HDAC2 (**B**), HDAC3 (**C**), HDAC4 (**D**), HDAC6 (**E**), HDAC8 (**F**) and HDAC9 (**G**) and the transcript levels (**H**) of ADIPOR1, CD300A, miR-155-5p, PTPN2, SARM1 and SOCS1 in the hippocampus in POCD. The data are presented as the mean \pm standard error of the mean from three individual experiments. *p<0.05 vs. the NC group.

affected by neuroinflammation, and the transcription of HDACs in hippocampal neurons is impacted by POCD. The opposite tendencies of HDACs and SIRT1 expression in POCD suggest that Class III HDACs may play roles opposite those of Class I and Class II HDACs with regard to neuroprotective effects²¹. However, the enzymatic activity rather than the protein expression of HDACs determines the function of these transcriptional regulators, especially upon HDACi treatment.

Expression of inflammatory cytokines may be induced by activation of microglial cells in the hippocampus and that peripheral immune cells may further cause a proinflammatory effect during POCD development. Once the initial microglia-mediated inflammation is alleviated, subsequent extensive proinflammation is quenched due to the shielding effect of the blood-brain barrier9. In the present study, pretreatment with Class I HDACis efficiently relieved the inflammatory effects better than pretreatment with Class II HDACis (Figure 3, 4C). Based on these outcomes, we determined that Class I HDACs, especially HDAC1, HDAC2 and HDAC8, are likely to contribute to regulating the transcription of genes involved in the inflammatory regulatory network.

Strictly speaking, the JAK/STAT and NF-κB/ p65 signaling pathways overlapped little (Figure 4A), although they can both result in inflammatory activation. In this study, we determined that neuroinflammation in POCD is coordinately regulated by multiple pathways and that the particular binding motif of Class I HDACs covers most genes in these three pathways (Figure 4D-F). Moreover, we also revealed that HDACs primarily occupy the promoters of negative inflammatory regulators and negatively regulate their transcription (Figure 5). These findings suggest that the enriched and activated Class I HDACs suppress the expression of negative factors of inflammation, thereby enhancing the inflammatory effect of POCD in the hippocampus; however, Class I HDACis can reverse this process and repress the enhanced inflammatory effect to prevent further nerve injury in POCD.

This study reverse-traced all the genes associated with inflammation from the Gene Ontology database and employed published ChIP-seq data to compare the common targets of HDACs. This is a novel approach for screening of target genes associated with diseases without high-throughput sequencing.

Conclusions

Taken together, our results provide evidence that specific inhibitors of Class I HDACs are potential therapeutic agents for POCD prevention and treatment *via* neuroinflammation inhibition.

Conflict of Interest

The Authors declare that they have no conflict of interests.

Acknowledgements

Chuanxin Yang performed all the experiments and analyzed the data. Fang Bao and Jiang Zhong helped prepare the POCD mouse model. Long Zhang and LiBing Deng analyzed the ChIP-seq and drew the corresponding figures. Qin Sha helped perform ChIP-qPCR. Hui Jiang designed this study and drafted and revised the manuscript. This project was supported by the Science & Technology Commission of Jinshan District, Shanghai (Grant No. 2017-3-09). The authors declare that there are no conflicts of interest.

References

- WANG W, WANG Y, Wu H, LEI L, Xu S, SHEN X, GUO X, SHEN R, XIA X, LIU Y, WANG F. Postoperative cognitive dysfunction: current developments in mechanism and prevention. Med Sci Monit 2014; 20: 1908-1912.
- TACHIBANA S, HAYASE T, OSUDA M, KAZUMA S, YAMAKAGE M. Recovery of postoperative cognitive function in elderly patients after a long duration of desflurane anesthesia: a pilot study. J Anesth 2015; 29: 627-630.
- ZHANG Y, BAO H G, Lv Y L, SI Y N, HAN L, WANG H Y, GAO Y J, JIANG W Q, ZHANG C. Risk factors for early postoperative cognitive dysfunction after colorectal surgery. BMC Anesthesiol 2019; 19: 6.
- 4) LIU Y, PAN N, MA Y, ZHANG S, GUO W, LI H, ZHOU J, LIU G, GAO M. Inhaled sevoflurane may promote progression of amnestic mild cognitive impairment: a prospective, randomized parallel-group study. Am J Med Sci 2013; 345: 355-360.
- YANG Z Y, YUAN C X. IL-17A promotes the neuroinflammation and cognitive function in sevoflurane anesthetized aged rats via activation of NF-kappaB signaling pathway. BMC Anesthesiol 2018; 18: 147.
- Li X, Sun Y, Jin Q, Song D, Diao Y. Kappa opioid receptor agonists improve postoperative cognitive dysfunction in rats via the JAK2/STAT3 signaling pathway. Int J Mol Med 2019; 44: 1866-1876.
- 7) Lu S M, Yu C J, Liu Y H, Dong H Q, Zhang X, Zhang S S, Hu L Q, Zhang F, Qian Y N, Gui B. S100A8 contributes to postoperative cognitive dysfunction in mice undergoing tibial fracture surgery by activating the TLR4/MyD88 pathway. Brain Behav Immun 2015; 44: 221-234.

- Wu Y, Dou J, Wan X, Leng Y, Liu X, Chen L, Shen Q, Zhao B, Meng Q, Hou J. Histone deacetylase inhibitor MS-275 alleviates postoperative cognitive dysfunction in rats by inhibiting hippocampal neuroinflammation. Neuroscience 2019; 417: 70-80.
- ZHU H, LIU W, FANG H. Inflammation caused by peripheral immune cells across into injured mouse blood brain barrier can worsen postoperative cognitive dysfunction induced by isoflurane. BMC Cell Biol 2018; 19: 23.
- VORHEES C V, WILLIAMS M T. Morris water maze: procedures for assessing spatial and related forms of learning and memory. Nat Protoc 2006; 1: 848-858
- 11) YANG Q, Fu C, ZHANG X, ZHANG Z, ZOU J, XIAO J, YE Z. Adiponectin protects against uric acidinduced renal tubular epithelial inflammatory responses via the AdipoR1/AMPK signaling pathway. Int J Mol Med 2019; 43: 1542-1552.
- 12) VALIATE B V S, ALVAREZ R U, KARRA L, QUEIROZ-JUNIOR C M, AMARAL F A, LEVI-SCHAFFER F, TEIXEIRA M M. The immunoreceptor CD300a controls the intensity of inflammation and dysfunction in a model of Ag-induced arthritis in mice. J Leukoc Biol 2019; 106: 957-966.
- 13) ZHOU X, YAN T, HUANG C, XU Z, WANG L, JIANG E, WANG H, CHEN Y, LIU K, SHAO Z, SHANG Z. Melanoma cell-secreted exosomal miR-155-5p induce proangiogenic switch of cancer-associated fibroblasts via SOCS1/JAK2/STAT3 signaling pathway. J Exp Clin Cancer Res 2018; 37: 242.
- 14) Li Y, Zhou H, Li Y, Han L, Song M, Chen F, Shang G, Wang D, Wang Z, Zhang W, Zhong M. PTPN2 improved renal injury and fibrosis by suppressing

- STAT-induced inflammation in early diabetic nephropathy. J Cell Mol Med 2019; 23: 4179-4195.
- 15) PRATHAB BALAJI S, VIJAY CHAND C, JUSTIN A, RAMANA-THAN M. Telmisartan mediates anti-inflammatory and not cognitive function through PPAR-gamma agonism via SARM and MyD88 signaling. Pharmacol Biochem Behav 2015; 137: 60-68.
- 16) DEINER S, LIU X, LIN H M, JACOBY R, KIM J, BAXTER M G, SIEBER F, BOOCKVAR K, SANO M. Does postoperative cognitive decline result in new disability after surgery? Ann Surg 2020. doi: 10.1097/ SLA.000000000000003764. Epub ahead of print].
- LIU X, YU Y, ZHU S. Inflammatory markers in postoperative delirium (POD) and cognitive dysfunction (POCD): a meta-analysis of observational studies. PLoS One 2018; 13: e0195659.
- 18) Kong ZH, Chen X, Hua H P, Liang L, Liu LJ. The oral pretreatment of glycyrrhizin prevents surgery-induced cognitive impairment in aged mice by reducing neuroinflammation and alzheimer's-related pathology via hmgb1 inhibition. J Mol Neurosci 2017; 63: 385-395.
- TAKASE K, ODA S, KURODA M, FUNATO H. Monoaminergic and neuropeptidergic neurons have distinct expression profiles of histone deacetylases. PLoS One 2013; 8: e58473.
- 20) AUNE S E, HERR D J, KUTZ C J, MENICK D R. Histone deacetylases exert class-specific roles in conditioning the brain and heart against acute ischemic injury. Front Neurol 2015; 6: 145.
- 21) Zhang Y, Anoopkumar-Dukie S, Arora D, Davey A K. Review of the anti-inflammatory effect of SIRT1 and SIRT2 modulators on neurodegenerative diseases. Eur J Pharmacol 2020; 867: 172847.